Applied Physics Letters ARTICLE scitation.org/journal/apl

Charge collection and trapping mechanisms in hexagonal boron nitride epilayers

Cite as: Appl. Phys. Lett. **119**, 221111 (2021); doi: 10.1063/5.0074409
Submitted: 8 October 2021 · Accepted: 20 November 2021 ·
Published Online: 2 December 2021

M. Almohammad, J. Li, J. Y. Lin, and H. X. Jiang[a)]

AFFILIATIONS

Department of Electrical and Computer Engineering, Texas Tech University, Lubbock, Texas 79409, USA

[a)]Author to whom correspondence should be addressed: hx.jiang@ttu.edu

ABSTRACT

Understanding charge collection and trapping mechanisms is crucial for using hexagonal boron nitride (*h*-BN) as active layers for many photonic and electronic devices such as deep UV detectors and emitters, neutron detectors, and single photon emitters. Charge collection and trapping mechanisms in *h*-BN epilayers have been investigated by probing impurity related optical emissions under an applied electrical field. Our results suggested that the existence of oxygen impurities affects the charge collection efficiency and results in an additional emission peak at 3.75 eV, corresponding to a donor-acceptor pair (DAP) recombination involving O_N (oxygen residing on the nitrogen site) donors and the V_B-H (boron vacancy bonded with hydrogen complex) deep level acceptors. Experimental results further revealed that the applied electric field induces an anti-correlation between the emission intensity of the DAP transition and the charge collection efficiency from which it was shown that it is possible to find an expression to quantitatively measure the maximum charge collection efficiency in *h*-BN. The results introduce not only a coherent picture for the relationship between common impurities in *h*-BN and charge collection and trapping mechanisms but also useful insights into possible approaches to improve the quality, purity, and charge collection of the *h*-BN epilayers.

Published under an exclusive license by AIP Publishing. https://doi.org/10.1063/5.0074409

Hexagonal boron nitride (h-BN) has recently received a lot of attention because of its extraordinary properties including wide bandgap ($E_g > 6$ eV),[1–4] high thermal neutron capture cross section,[5,6] high optical absorption and emission efficiency,[1–4,7–11] and excellent chemical and thermal stability.[12] As such, h-BN has been extensively investigated for technologically important device applications ranging solid-state neutron detectors,[13–20] single photon emitters,[21–23] and deep UV emitters[10] and detectors[11] as well as for probing fundamental properties of deep UV optoelectronic materials.[1–4,7–9]

Due to its ultra-wide bandgap, *h*-BN possesses an extremely high electrical resistivity ($\rho > 10^{13}\,\Omega\cdot$cm),[15,18] making it difficult to extract its basic electrical parameters and properties. Measuring the combined mobility-lifetime product ($\mu\tau$) under photoexcitation has been an effective method to characterize the purity and quality of the material.[19–23] Under an above bandgap photoexcitation and applied electric field, $\mu\tau$ can be determined by measuring and analyzing the photocurrent-voltage characteristics via the classical Many's equation.[24] Another important transport parameter that can be extracted from such measurements is the surface recombination field, which is the ratio of the surface recombination velocity to the carrier mobility (s/μ).

For any active device using *h*-BN, especially deep UV detectors and emitters and neutron detectors, it is important to understand how charge carriers are being excited, trapped, and collected. It has been known through the performance of neutron detectors that only part of neutron generated charge carriers are collected by electrodes, whereabouts of the remaining uncollected charge carriers are still not exactly known. Here, we report studies of charge carrier generation, trapping, and collection by probing impurity optical emissions under different applied electric fields.

h-BN epilayers (*h*-BN) employed in this study were synthesized by metal-organic chemical vapor deposition (MOCVD) using triethylboron (TEB) and ammonia (NH_3) as the precursors for B and N, respectively. Hydrogen was used as a carrier gas. The basic layer of *h*-BN epilayers is shown in Fig. 1(a). Due to the lattice constant mismatch of *h*-BN and sapphire,[25,26] a low temperature *h*-BN buffer layer of about 20 nm in thickness was first deposited on *c*-plane sapphire at 800 °C. This was then followed by the growth of a 1 μm thick *h*-BN at a growth temperature of 1600 °C. A shadow mask was used for metal deposition to form metal contacts on the two sides of *h*-BN epilayers. Ohmic contacts consisting of bilayers of Ni/Au (100/110 nm) were deposited by e-beam deposition. The dimension of the *h*-BN layer is

Published under an exclusive license by AIP Publishing

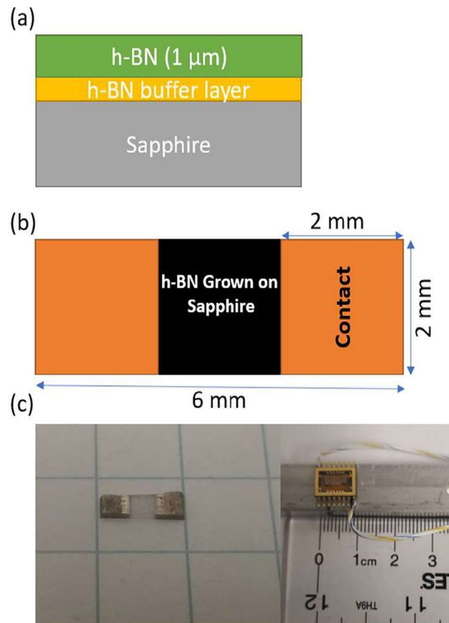

Fig. 1

FIG. 1. Sample used in this study: (a) A schematic of the layer structure of the *h*-BN epilayer, (b) top view showing the dimensions of the *h*-BN layer with Ohmic contacts, and (c) photo images of the *h*-BN sample and the fabricated structure.

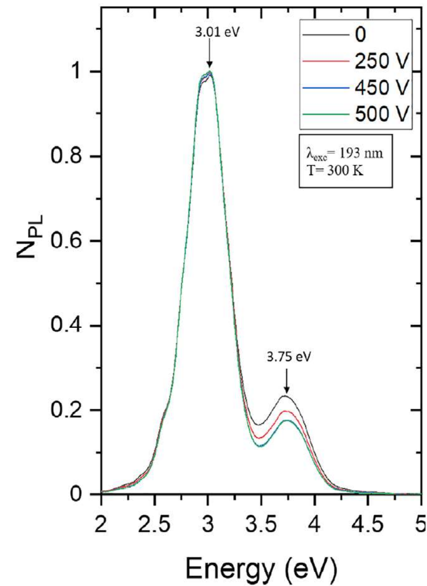

Fig. 2

FIG. 2. Room temperature normalized PL spectra (N_{PL}) measured at four representative applied voltages under 193 nm laser excitation. Each emission spectrum is normalized to the 3.01 eV emission peak at zero bias voltage.

6 mm × 2 mm with metal contacts of 2 mm in width and length, and the spacing between the metal contacts is 2 mm as shown in Fig. 1(b). Wire bonding was used to connect the metal contacts to a semiconductor device package as shown in Fig. 1(c). For the photoluminescence (PL) measurements, a pulsed excimer laser emitting at 193 nm was used as an excitation source, and the PL emission spectra were collected using an optical fiber coupled with a monochromator (Ocean Optics USB2000+). It is well known that the optical absorption length of the above bandgap photons in *h*-BN is only about 14 nm.[11] Thus, the PL setup ensured that no excitation photons can penetrate into sapphire. A source meter was used to supply different bias voltages to *h*-BN epilayers corresponding to applied electric fields (E) varying from 0 to 2.5 kV/cm. A focusing lens and a long wavelength-pass filter were utilized to focus the pulsed laser beam onto the sample and attenuate the laser line intensity as well as the band edge emission on the spectrometer side, respectively.

Figure 2 plots the normalized room temperature PL spectra measured with four representative applied voltages. The PL emission spectra plotted in Fig. 2 were normalized to the 3.01 eV emission peak at zero bias voltage. Two dominant emission lines at 3.01 and 3.75 eV were observed. We also checked PL emission from the sapphire substrate only and no such peaks were present. The intensity of the 3.01 eV emission line is hardly changed when the applied electric field is increased, while the intensity of the 3.75 eV emission line clearly decreases with an increase in the applied electric field. On the other hand, when the applied bias voltages approach values close to 500 V, the intensity of the 3.75 eV emission line saturates and does not approach to zero with a further increase in the applied electric field. This can be clearly observed from Fig. 2 that the PL spectra acquired at V_b = 450 and 500 V are almost identical and cannot be distinguished. When using *h*-BN as a detector material, the charge collection efficiency and hence the detection efficiency are expected to increase with increasing of the applied bias voltage. The observed systematic dependence of the emission intensity of the impurity related emission line at 3.75 eV on the applied bias voltage suggests that it is possible to establish a relationship between the PL emission intensity and the charge collection efficiency (η_C) in *h*-BN.

Under light excitation, the total number of photo-generated carriers is N_t. A fraction of these photo-generated carriers, N_e, is being collected by the electrodes and contributes to the electrical signal. However, another portion of these photo-generated carriers, N_o, is trapped by impurities or defects, which contributes to the observed optical emission. The relationship among N_t, N_e, and N_o should follow as:

$$N_t = N_e + N_o. \tag{1}$$

The PL intensity (I_{emi}) of the 3.75 eV impurity emission line is proportional to the number of trapped carriers, which contributed to the optical channel (N_o), $I_{emi} \propto N_o$, and thus, $I_{emi} = A \cdot N_o$, where A is a proportionality constant. Under an applied electric field E, we have $I_{emi}(E) = A \cdot N_o(E)$. The normalized emission intensity, N_{PL} is, thus,

$$N_{PL} = \frac{N_o(E)}{N_o(E=0)}. \tag{2}$$

On the other hand, the total number of photo-generated charge carriers is independent of the applied electric field and depends only on the excitation light intensity. Therefore, we have

Published under an exclusive license by AIP Publishing

$$N_t = N_e(E) + N_o(E) = N_e(E=0) + N_o(E=0). \quad (3)$$

It is expected that the number of collected charge carriers contributing to the electrical signal, $N_e(E)$, increases while the number of charge carriers trapped by the impurities giving rise to the observe PL emission line, $N_o(E)$, decreases with an increase in the applied electric field, or equivalently $\frac{dN_e(E)}{dE} > 0$, $\frac{dN_o(E)}{dE} < 0$, and $\frac{dN_o(E)}{dE} = -\frac{dN_e(E)}{dE}$. However, $N_e = 0$ at $E = 0$ since no charge carriers can be collected at zero bias voltage. In this analysis, we neglected possible variations of exciton generation and recombination with applied electric fields. Consequently, we have

$$N_o(E=0) = N_t. \quad (4)$$

Dividing Eq. (1) by N_t, we get $N_e(E)/N_t + N_o(E)/N_t = 1$ or

$$\eta_c + \frac{N_o(E)}{N_t} = 1. \quad (5)$$

Here, $\eta_c = N_e(E)/N_t$ defines the charge collection efficiency. Combining Eqs. (2)–(5) yields that

$$\eta_c = 1 - \frac{N_o(E)}{N_t} = 1 - \frac{N_o(E)}{N_o(E=0)} = 1 - N_{PL}. \quad (6)$$

Equation (6) establishes that the charge collection efficiency can be determined via the normalized PL emission intensity, N_{PL}, of an impurity transition.

Figure 3 plots (1-N_{PL}) of the 3.75 eV emission line, or equivalently, the charge collection efficiency, η_c, as a function of the applied electric field under 193 nm excitation. The values of (1-N_{PL}) of the 3.75 eV emission line increase with an increase in the applied electric field and approach to a saturation value at higher applied electric fields. From the optical process perspective, when the applied electric field is increased, more charge carriers can reach the electrodes for collection and fewer charge carriers can participate in the radiative optical transition and hence the PL emission intensity is reduced, as shown in Fig. 2. Since (1-N_{PL}) defines the charge collection efficiency at an applied electric field E, (1-N_{PL}) vs E plot is expected to resemble the photocurrent-voltage (I-V) characteristics of an *h*-BN detector[27] and be described by Many's equation.[24] In Fig. 3, the red solid curve is the least squares fit of measured data (black square) with a modified Many's equation[24] as described below

$$(1 - N_{PL}) = \eta_{c,i}(V) = A\left[\frac{V\mu_i\tau_i\left(1 - e^{-\frac{L^2}{V\mu_i\tau_i}}\right)}{L^2\left(1 + \frac{s_i L}{\mu_i V}\right)}\right], \quad (i = e, h), \quad (7)$$

where $\mu\tau$ and s/μ represent the charge carrier mobility-lifetime product and the surface recombination field, respectively and $\eta_c(V)$ denotes the charge collection efficiency by the electrodes at a bias voltage of V (=E·L) with E being the applied electric field and L being the width of the *h*-BN device (2 mm in the present case).

With increasing of the applied electric field, from the electrical transport perspective, the number of charge carriers being collected by the electrodes will increase, whereas the number of trapped charge carriers will decrease. An increase in the number of trapped charge carriers will increase the impurity PL emission intensity but will reduce the number of charge carriers being collected by the electrodes. Therefore, any decrease in the PL emission intensity of the impurity transition is, thus, anticorrelated with an increase in the charge collection efficiency.

The fitting between the experimental data and Eq. (7) yields a mobility-lifetime product ($\mu\tau$) of 1.3×10^{-4} cm^2/V for electrons and s/μ (surface recombination field) of 7.3×10^2 V/cm. It should be noted that not only we find the correlation between the optical emission intensity involving an impurity transition and charge collection efficiency, but also we find an effective method to determine the maximum charge collection efficiency for a given device, which is constant A in Eq. (7). For the *h*-BN device studied here, we have A = 46.3 %. In the past, the I-V characteristics under photoexcitation have been widely utilized to extract the information concerning the electrical transport properties, including the charge carrier mobility-lifetime product ($\mu\tau$) and the surface recombination field (s/μ), via the use of the classical Many's equation[24]

$$I(V) = I_{o,i}[\eta_{c,i}] = I_{o,i}\left[\frac{V\mu_i\tau_i\left(1 - e^{-\frac{L^2}{V\mu_i\tau_i}}\right)}{L^2\left(1 + \frac{s_i L}{\mu_i V}\right)}\right], \quad (i = e, h), \quad (8)$$

where I_o is defined as the saturation current, which depends on multiple factors such as excitation light intensity, charge carrier excitation efficiency, and mobility of charge carriers (μ). It is important to note that while one can extract important transport properties such as $\mu\tau$ and s/μ from the photocurrent-voltage characteristics,[26,27] the critical device performance parameter of charge collection efficiency (η_c)

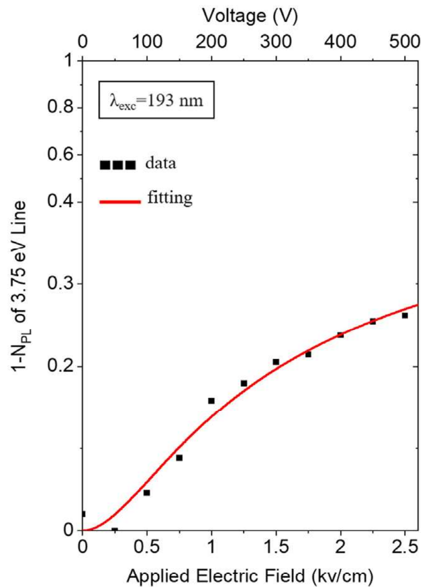

FIG. 3. Plot of (1-N_{PL}) of the 3.75 eV emission line as a function of the applied electric field under 193 nm excitation, where N_{PL} is the relative emission intensity after normalized to the 3.01 eV emission peak at zero bias voltage. The solid squares are measured values of (1-N_{PL}), and the solid curve is the least squares fit of data with Eq. (7).

Published under an exclusive license by AIP Publishing

cannot be directly acquired from such measurements because I_o in Eq. (8) has no physical meaning.

The observed emission peak at 3.75 eV is most likely corresponding to a donor-acceptor pair (DAP) transition based on the nature of its broad emission spectral linewidth and below energy bandgap emission. A recent theoretical study revealed that oxygen impurities occupying the nitrogen sites (O_N) act as donors, whereas boron vacancy-hydrogen complexes (V_B-H) are acceptor-like deep level defects in *h*-BN.[28] Therefore, one of the most probable impurity candidates involved in the 3.75 eV emission line is oxygen impurities, which were introduced into *h*-BN during high temperature MOCVD growth because of the use of the sapphire substrate.[19] During MOCVD growth, due to the incorporation of O_N donor impurities, the Fermi level in *h*-BN will move toward the conduction band edge. This, in turn, will reduce the formation energy and enhance the incorporation of (V_B-H) acceptor-like defects.[28] It is, thus, highly plausible that (V_B-H) acceptors and O_N donors are the physical origins of the observed DAP emission line at 3.75 eV. While the origin of 3.01 eV is not clear at this point, the same theoretical calculation indicated that the energy level of oxygen interstitial defects ($O_i^{0,-2}$) in *h*-BN is located at 3.01 eV below the conduction band.[28] Therefore, it is conceivable that the 3.01 eV emission line is related to O_i, which, however, is too deep to be affected by the applied electric field.

In thick *h*-BN epilayers (~50 μm) grown at lower temperatures (~1500 °C) with long growth times,[19] an additional emission peak in the PL emission spectrum, possibly corresponding to a DAP recombination involving the O_N donor and the C_N (carbon occupying nitrogen sites), has been observed. Carbon impurities have a binding energy of about 2.3 eV above the valence band, which in conjunction with O_N may have contributed to a broad emission line in *h*-BN at about 3.5 eV.[19]

Based on the above discussion, it can be envisioned that oxygen impurities can trap the photoexcited electrons and increase the emission intensity of the DAP transition at 3.75 eV and subsequently reduce the charge collection efficiency. An applied electric field will reduce the number of the photoexcited electrons being trapped by the oxygen impurities; therefore, the emission intensity of the transition line at 3.75 eV involving O_N donors is reduced in favor of increasing the charge collection efficiency.

The energy level of oxygen impurities (O_N) in *h*-BN has been previously calculated to be ~0.61 eV below the conduction band edge.[28] The calculated energy level of (V_B-H) acceptors in *h*-BN is ~1.65 eV above the valence band edge.[28] These previous results together with the observed PL emission peak position at 3.75 eV attributing to the (O_N) − (V_B-H) DAP transition enable the construction of an energy band diagram, including the energy bandgap, E_g, O_N donor energy level, and V_B-H acceptor energy level in *h*-BN epilayers, which is shown in Fig. 4. The results also provide a room temperature bandgap of *h*-BN of ~6.01 eV.

We believe that there is a need for additional studies aimed at achieving improved understanding of mechanisms of various impurity transitions in *h*-BN to provide insights into further improvement of *h*-BN materials and devices. However, the present study not only provides useful insights into the plausible mechanism of the observed 3.75 eV transition line but also yields an effective method for determining the charge collection efficiency, which is critically important for further advancing *h*-BN detector development.

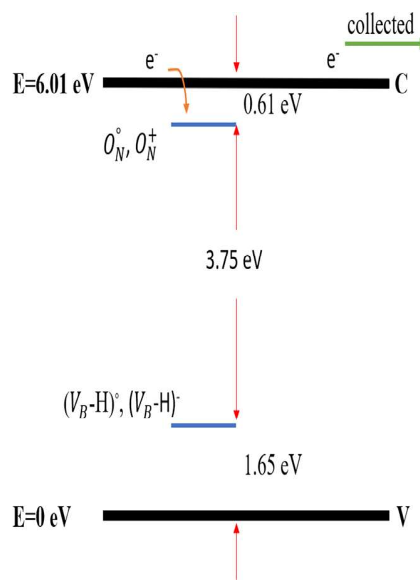

FIG. 4. Energy band diagram including the energy bandgap E_g, O_N donor energy level, and (V_B-H) acceptor energy level in *h*-BN epilayers.

In summary, charge collection and trapping mechanisms have been investigated in *h*-BN epilayers grown on the sapphire substrate by MOCVD. It was found that the emission intensity of an impurity transition at 3.75 eV is anti-correlated with the charge collection efficiency, signifying that increasing the applied electric field leads to an increase in the charge collection efficiency and a decrease in the emission intensity of the impurity transition at 3.75 eV. Based on previous experimental and theoretical studies, we attributed the observed emission line at 3.75 eV to a DAP recombination, involving the O_N (oxygen residing on nitrogen sites) donors and the V_B-H (boron vacancy bonded with hydrogen) deep level acceptors. The presence of oxygen impurities not only introduces additional emission lines but strongly affects the charge collection efficiency of *h*-BN detectors. These results also provide an improved understanding of the impurity/defect formation during the growth process and their effects on the electrical and optical properties of *h*-BN epilayers. Further improvements in the material quality of *h*-BN are required to minimize the concentrations of dominant defects, including O_N and V_B-H impurities, and to enhance the charge collection efficiency of *h*-BN devices. With the identification of these common defects, it is feasible to eliminate them through growth techniques including optimization of the buffer layer conditions or insertion of multiple intermediate layers prior to the deposition of high temperature *h*-BN epilayers.

This work was supported by DOE ARPA-E (Grant Nos. DE-AR0000964 and DE-AR0001257). H.X.J. and J.Y.L. are grateful to the AT&T Foundation for the support of Ed Whitacre and Linda Whitacre endowed chairs.

AUTHOR DECLARATIONS

Conflict of Interest

The authors have no conflicts to disclose.

Published under an exclusive license by AIP Publishing

DATA AVAILABILITY

The data that support the findings of this study are available from the corresponding author upon reasonable request.

REFERENCES

[1] A. Zunger, A. Katzir, and A. Halperin, Phys. Rev. B **13**, 5560 (1976).
[2] T. Sugino, K. Tanioka, S. Kawasaki, and J. Shirafuji, Jpn. J. Appl. Phys. Part 2 **36**, L463 (1997).
[3] K. Watanabe, T. Taniguchi, and H. Kanda, Nat. Mater. **3**, 404 (2004).
[4] X. Z. Du, J. Li, J. Y. Lin, and H. X. Jiang, Appl. Phys. Lett. **111**, 132106 (2017).
[5] G. F. Knoll, *Radiation Detection and Measurement*, 4th ed. (John Wiley & Sons, 2010).
[6] O. Osberghaus, Z. Phys. **128**, 366 (1950).
[7] K. Watanabe and T. Taniguchi, Phys. Rev. B **79**, 193104 (2009).
[8] X. K. Cao, B. Clubine, J. H. Edgar, J. Y. Lin, and H. X. Jiang, Appl. Phys. Lett. **103**, 191106 (2013).
[9] B. Huang, X. K. Cao, H. X. Jiang, J. Y. Lin, and S. H. Wei, Phys. Rev. B **86**, 155202 (2012).
[10] S. Majety, X. K. Cao, J. Li, R. Dahal, J. Y. Lin, and H. X. Jiang, Appl. Phys. Lett. **101**, 051110 (2012).
[11] J. Li, S. Majety, R. Dahal, W. P. Zhao, J. Y. Lin, and H. X. Jiang, Appl. Phys. Lett. **101**, 171112 (2012).
[12] Z. Liu, Y. Gong, W. Zhou, L. Ma, J. Yu, J. C. Idrobo, J. Jung, A. H. MacDonald, R. Vajtai, J. Lou, and P. M. Ajayan, Nat. Commun. **4**, 2541 (2013).
[13] T. C. Doan, J. Li, J. Y. Lin, and H. X. Jiang, AIP Adv. **6**, 075213 (2016).
[14] J. Li, R. Dahal, S. Majety, J. Y. Lin, and H. X. Jiang, Nucl. Inst. Methods Phys. Res. A **654**, 417 (2011).
[15] A. Maity, S. J. Grenadier, J. Li, J. Y. Lin, and H. X. Jiang, J. Appl. Phys. **123**, 044501 (2018).
[16] A. Maity, S. J. Grenadier, J. Li, J. Y. Lin, and H. X. Jiang, J. Appl. Phys. **125**, 104501 (2019).
[17] A. Maity, S. J. Grenadier, J. Li, J. Y. Lin, and H. X. Jiang, Appl. Phys. Lett. **114**, 222102 (2019).
[18] A. Maity, S. J. Grenadier, J. Li, J. Y. Lin, and H. X. Jiang, Appl. Phys. Lett. **116**, 142102 (2020).
[19] S. J. Grenadier, A. Maity, J. Li, J. Y. Lin, and H. X. Jiang, Appl. Phys. Lett. **112**, 162103 (2018).
[20] S. J. Grenadier, A. Maity, J. Li, J. Y. Lin, and H. X. Jiang, Appl. Phys. Lett. **115**, 072108 (2019).
[21] R. Bourrellier, S. Meuret, A. Tararan, O. Stephan, M. Kociak, L. H. G. Tizei, and A. Zobelli, Nano Lett. **16**, 4317 (2016).
[22] T. Q. P. Vuong, G. Cassabois, P. Valvin, A. Ouerghi, Y. Chassagneux, C. Voisin, and B. Gil, Phys. Rev. Lett. **117**, 097402 (2016).
[23] T. Tran, K. Bray, M. J. Ford, M. Toth, and I. Aharonovich, Nat. Nanotechnol. **11**, 37 (2016).
[24] A. Many, J. Phys. Chem. Solids **26**, 575 (1965).
[25] X. Z. Du, J. Li, J. Y. Lin, and H. X. Jiang, Appl. Phys. Lett. **108**, 052106 (2016).
[26] A. Maity, T. C. Doan, J. Li, J. Y. Lin, and H. X. Jiang, Appl. Phys. Lett. **109**, 072101 (2016).
[27] J. Li, A. Maity, S. J. Grenadier, J. Y. Lin, and H. X. Jiang, Appl. Phys. Lett. **118**, 092102 (2021).
[28] L. Weston, D. Wickramaratne, M. Mackoit, A. Alkauskas, and C. G. Van de Walle, Phys. Rev. B **97**, 214104 (2018).

Published under an exclusive license by AIP Publishing